

Mott transition in the Hubbard model on the hyper-kagome lattice

Hunpyo Lee and Hartmut Monien

Bethe Center for Theoretical Physics, Universität Bonn, 53115 Bonn, Germany

(Dated: March 17, 2009)

Motivated by recent experiment on the $\text{Na}_4\text{Ir}_3\text{O}_8$ compound we study the Hubbard model on the “hyper-kagome lattice”, which forms a three-dimensional network of corner sharing triangles, using dynamical cluster approximation (DCA) method with $N_c=12$ combined with the continuous-time quantum Monte Carlo (CT QMC) method. The system undergoes a Mott transition if the Hubbard interaction U/W (W is the bandwidth) exceeds the value of 1.2 for $T=0.1$ and displays reentrant behavior due to competition between the magnetic correlation and the kinetic energy of electrons due to the geometrical frustration. We observe a “critical slowing down” of the double occupancy which shows evidence of a continuous transition. The nearest-neighbor and next nearest-neighbor spin-spin correlations indicate a paramagnetic metallic state in the weak-coupling regime and an antiferromagnetic (AF) Mott insulator in the strong-coupling regime within the temperature range which we can access with our numerical tools.

PACS numbers: 71.10.Fd

Frustrated electronic systems exhibit a wide range of phases due to competition between strong electronic correlations and geometric frustration. The $\text{Na}_4\text{Ir}_3\text{O}_8$ compound with a $S=1/2$ three-dimensional network of corner sharing triangles, which is called the “hyper-kagome lattice”, was discovered.¹ Due to the structure of corner sharing triangles, the system displays the electronic correlations and geometric frustration at the same time. Each tetrahedron in the pyrochlore lattice, which is shown in Fig. 1, consists of Ir (indicated as “filled” circles) and Na (indicated as “empty” circles). $S=1/2$ spins are carried through Ir^{4+} on the hyper-kagome lattice (blue lines in Fig. 1) because Ir is tetravalent with five electrons in $5d$ orbitals. In recent experiment by Y. Okamoto (Ref. 1), a spin liquid state at low temperature was found. Theoretical work, related to this experiment, has mostly addressed the strong-coupling limit using the Heisenberg model^{2,3,4,5,6}. These papers concentrated on the nature of the ground state which was identified as the spin liquid state. Even more recently, it was shown experimentally that this material undergoes a transition to a metallic state under pressure⁷.

The two important theoretical questions which we will address in this Letter are if the phase diagram shows a reentrant Mott phase with a first-order transition as was found for the anisotropic triangular lattice¹⁸ and if the spin liquid state is stable at finite temperatures. The dynamical mean field theory (DMFT)^{8,9} is a successful method to describe the Mott transition. However, since the single-site DMFT ignores the spatial fluctuations, the system becomes metallic as temperature is decreased. This behavior is quite different from the phase diagram obtained from quantum Monte Carlo (QMC) on the triangular lattice.^{10,11} The cluster extension of the DMFT methods such as the dynamical cluster approximation (DCA)^{12,13,14} and the cellular dynamical mean field theory (CDMFT)¹⁵ were developed in order to consider the spatial fluctuations. In these methods the short range correlations are treated exactly within the cluster size, while the long range correlations are included on the

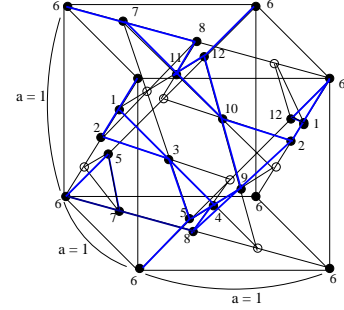


FIG. 1: In the pyrochlore lattice, “filled” circles and “empty” circles present Ir and Na, respectively. The blue lines show the hyper-kagome lattice of Ir. a is the lattice constant. Lattice points labeled by 1,2,...,12 represent relative positions in each unit cell.

mean field level only. The difference between both methods lies in the boundary condition of the cluster given by the Laue function¹². In this paper, we employ the DCA method combined with the continuous-time quantum Monte Carlo (CT QMC) method¹⁶ as cluster solver and measure the total density of states (DOS), double occupancy, nearest-neighbor and next nearest-neighbor spin-spin correlation functions.

We consider the Hubbard model on the hyper-kagome lattice at half-filling:

$$H = -t \sum_{\langle i,j \rangle \sigma} c_{i\sigma}^\dagger c_{j\sigma} + U \sum_i n_{i\uparrow} n_{i\downarrow}, \quad (1)$$

where $c_{i\sigma}$ ($c_{i\sigma}^\dagger$) is the annihilation (creation) operator of an electron with spin σ at the i -th site, t is the hopping

matrix element and U represents the Coulomb repulsion. We set $t=1.0$ and the bandwidth is $W=6t$. For the DCA method we consider an unit cell which has twelve sites ($N_c=12$) in the simple cubic lattice, as shown in Fig. 1. In the DCA method the Green's functions are determined by the self-consistency condition. We directly write the hopping matrix $T(\tilde{\mathbf{k}})$ with the periodic boundary condition in the real space. Here G_0 , Σ and $T(\tilde{\mathbf{k}})$ are described by 12×12 matrices. In this case the self-consistent equation for the DCA method is the same as for the CDMFT method except the hopping matrix $T(\tilde{\mathbf{k}})$:

$$G_0^{-1}(i\omega_n) = \left(\int d\tilde{\mathbf{k}} \frac{1}{i\omega_n + \mu - T(\tilde{\mathbf{k}}) - \Sigma(i\omega_n)} \right)^{-1} + \Sigma(i\omega_n), \quad (2)$$

where μ is the chemical potential and ω_n is the Matsubara frequency. The Brillouin zone of the superlattice also becomes simple cubic lattice with $\pi/a < k_x, k_y, k_z < \pi/a$, where $a = 1$ is the lattice constant and the summation of $\tilde{\mathbf{k}}$ is taken over the Brillouin zone of the superlattice. We use 8×10^6 $\tilde{\mathbf{k}}$ -points for integration of Eq. (2). We solve the quantum impurity problem using the CT QMC method. Unlike the Hirsch-Fye discrete time quantum Monte Carlo method¹⁷ which is carried out by the auxiliary Ising-like spins, the CT QMC method performs a random walk in the space of the perturbation expansion without Trotter decomposition error. The computational time of CT QMC scales as $\langle k \rangle \sim 0.5N_c U\beta$ and is therefore superior to the Hirsch-Fye quantum Monte Carlo method for which the computational time scales as $\langle k \rangle \sim 2N_c U\beta$, where $\langle k \rangle$ is the matrix size. We briefly summarize the CT QMC method. The main idea of CT QMC is to perform a diagram expansion of the partition function $Z = Z_0 e^{-U \int d\tau n_{\uparrow} n_{\downarrow}}$ in powers of the interaction U . In this case we can reexpress the partition function as

$$Z = \sum_k Z_0 \frac{(-U)^k}{k!} \int d\tau_1 \cdots d\tau_k \int \mathcal{D}[c, \bar{c}] < n_{\uparrow}(\tau_1) n_{\downarrow}(\tau_1) \cdots n_{\uparrow}(\tau_k) n_{\downarrow}(\tau_k) >, \quad (3)$$

where $< n_{\uparrow}(\tau_1) n_{\downarrow}(\tau_1) \cdots n_{\uparrow}(\tau_k) n_{\downarrow}(\tau_k) >$ is determined by the non-interacting Green's function and Wick's theorem and Z_0 is the unperturbed part. The interacting Green's functions are calculated by numerical averaging of Eq. (3). We use 3×10^6 QMC sweeps approximately and consider twenty-one Matsubara frequency points.

Now let us investigate the phase diagram of the hyperkagome lattice Hubbard model at half filling. In order to check the existence of a gap, we calculate the density of state (DOS) at the Fermi level ($\omega = 0$) by using the Pade approximation and the analytic form which is given by

$$G(\beta/2) \approx \frac{1}{\beta} \rho(\omega = 0), \quad (4)$$

where β is the inverse temperature and $\rho(\omega)$ is the density of states. Because Eq. (4) is satisfied at sufficiently low temperature, we employ the Pade approximation in $T > 0.1$ regions and compare the results of both

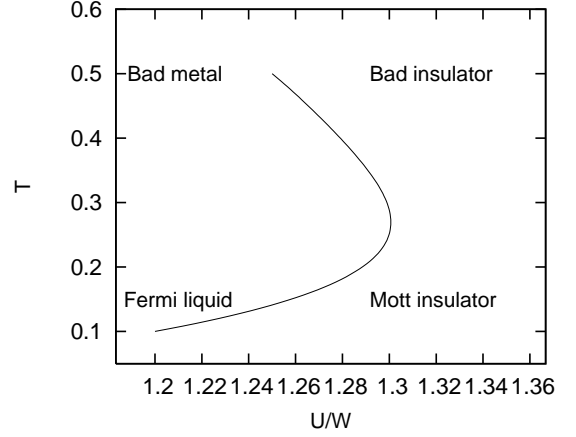


FIG. 2: Phase diagram of the Hubbard model on the hyperkagome lattice

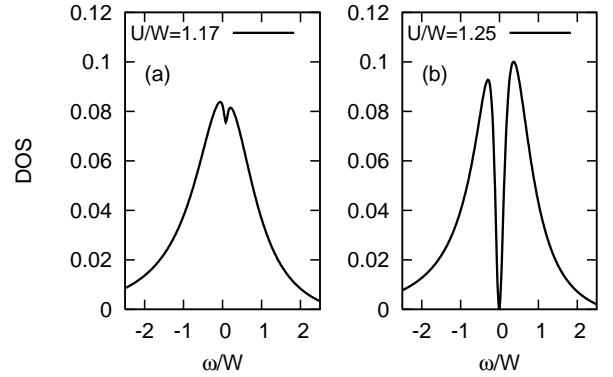


FIG. 3: The density of state corresponding to (a) $U/W=1.17$ and (b) $U/W=1.25$ for $T=0.1$. The Pade approximation is employed for analytical continuation

methods at $T=0.1$. The Pade approximation method for analytical continuation works well at the high temperature regime due to very small error in CT QMC method. Moreover, the results of Eq. (4) support those obtained from the Pade approximation at low temperature. The phase diagram in U - T plane is shown in Fig. 2. As temperature is decreased in the transition region ($U/W=1.28$) above $T=0.3$, the system prefers the metallic state due to the dominant low energy excitation of electrons. Below $T=0.2$ the system is strongly controlled not by itinerant electrons but by antiferromagnetic (AF) fluctuations, which are ignored in the single-site DMFT. Therefore, the Mott insulator lies in the low temperature regions. This results in a reentrant behavior which is also presented in the Hubbard model on the anisotropic triangular lattice¹⁸ related to the frustrated organic material κ -(BEDT-TTF)₂Cu[N(CN)₂]Cl^{19,20}. We analyze the DOS close to critical U/W at $T=0.1$ using Pade approximation for analytical continuation. The DOS for $U/W=1.17$ and $U/W=1.25$ is exhibited in Figs. 3(a)-(b). At $U/W=1.17$ a quasiparticle peak due to itinerant

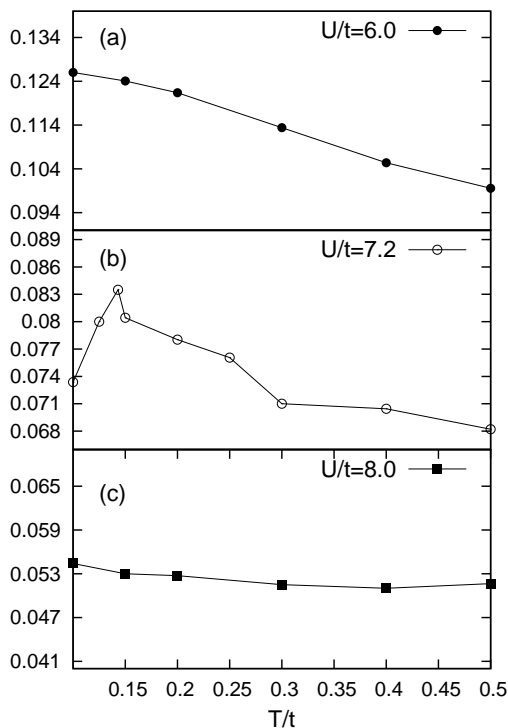


FIG. 4: Double occupancy as a function T for (a) $U/W=1.0$, (b) $U/W=1.2$ and (c) $U/W=1.333$.

of electrons is formed strongly around the Fermi level. At $U/W=1.25$ the DOS changes dramatically at the Fermi level and the system turns to a Mott insulator. We did not observe any evidence for the pseudogap formation like the results of kagome lattice²¹. The magnetic state is suppressed due to the geometrical frustration in contrast to the square lattice²². To investigate the character of Mott transition in more detail we present the double occupancy as a function of temperature for various interactions in Figs. 4(a)-(c). As temperature is decreased at weak interaction strength $U/W=1.0$ in Fig. 4(a), the double occupancy is increased. This means that the entropy due to kinetic energy of the dominant quasiparticles, is optimized by pushing the interaction in order to decrease the free energy. Non-monotonic dependence of the double occupancy is observed at intermediate interaction $U/W=1.2$ in Fig. 4(b). For $T > 0.3$ the system displays the insulating state due to effect of the dominant local magnetic moment. As temperature is decreased, it changes into the metallic state due to development of the quasiparticle. After passing the peak temperature $T_0=0.15$, at lower temperatures the system reenters the insulating state because the magnetic correlations get enhanced. This is indeed evidence for the reentrant behavior which is exhibited in geometrically frustrated systems like the case of Hubbard model on anisotropic triangular lattice. In Fig. 4(c), we see a small gradual increase in the double occupancy as temperature is decreased, reflecting a gain in kinetic energy. Our analysis

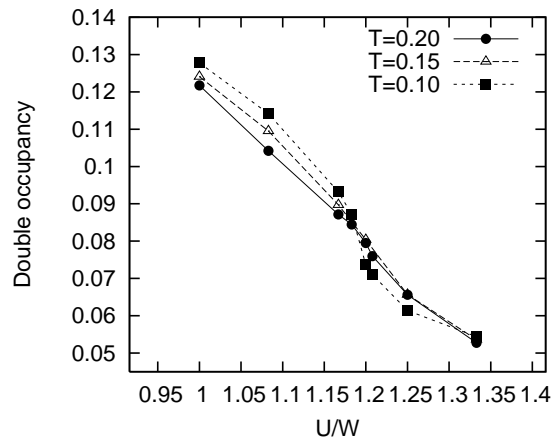


FIG. 5: Double occupancy as a function U/W for $T=0.2$ and $T=0.1$. There is a “critical slowing down” behavior at $T=0.1$ which represents the evidence of a continuous transition. $U_c/W=1.2$ for $T=0.1$

in the Fermi liquid region ($U/W=1.0$) and Mott insulator region ($U/W=1.33$) is similar to that obtained from the cluster-extension of DMFT method on the square lattice²³. We further investigate the double occupancy as function of interaction at various temperatures in order to see the type of transition. The result is shown in Fig. 5. As interaction is increased, at $T=0.2$ the double occupancy decreases smoothly because of the development of local magnetic moment. At $T=0.1$ the “critical slowing down” behavior is observed around $U_c/W=1.2$. This behavior is quite similar to the results of the fully frustrated Hubbard model which indicates a second-order transition in the single-site DMFT calculation²⁴. We suspect that there is a continuous transition in the Hubbard model on the hyper-kagome lattice. We calculate the nearest-neighbor $\langle S_i^z S_{i+1}^z \rangle$ and next nearest-neighbor spin-spin correlation $\langle S_i^z S_{i+2}^z \rangle$, which are shown in Fig 6. In the weak interaction regions the system displays paramagnetic metallic behavior, unlike the case of the square lattice which has strong AF correlations due to perfect nesting. As interaction is increased, there is a competition between the quasiparticle formation and the frustrated spin correlation. At $U_c/W=1.27$ for $T=0.2$ both the nearest-neighbor and next nearest-neighbor spin-spin correlations are enhanced at the same time. We find the AF Mott insulator in the strong interaction regions. We do not find a spin liquid state for $T > 0.1$.

Finally, we compare our results with those recently obtained from the mean-field calculation²⁵. In the mean-field calculation the system has continuous metal-insulator transition at critical interaction $U_c/W=1.03$. These results are comparable to our results with a continuous metal-insulator transition at $U_c/W=1.2$ for $T=0.1$.

In summary, we have presented results of DCA study combined with CT QMC method as a cluster solver in the Hubbard model on the hyper-kagome lattice. The

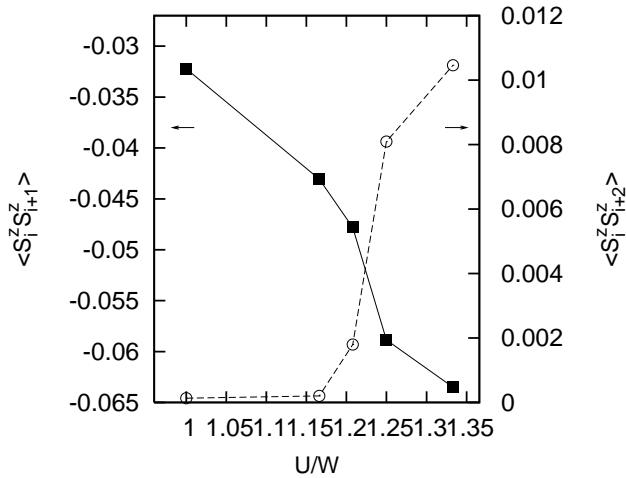


FIG. 6: The nearest-neighbor and next nearest-neighbor spin-spin correlation function as a function of U/W for $T=0.2$. Both spin-spin correlations are rapidly increased at $U_c/W=1.27$

phase diagram in the U - T plane has reentrant behavior due to geometrical frustration and is quite similar to that on the anisotropic triangular lattice. The difference of both lattice types is that while the hyper-kagome lattice exhibits a continuous transition, the anisotropic triangular lattice displays a first-order transition. Us-

ing Pade approximation for the analytical continuation we calculated the DOS close to critical $U_c/W=1.2$ for $T=0.1$. There is rapid change in the DOS at Fermi level. The formation of pseudogap is not observed because the magnetic fluctuations are suppressed. We investigated the double occupancy as a function of temperature and as a function of interaction U/W to study the nature of the Mott transition in more detail. For intermediate values of the interaction, the double occupancy as a function of temperature has non-monotonic behavior which represents the character of reentrant behavior. We also find the “critical slowing down” of the double occupancy as a function of interaction. We suspect that at low temperature there might be a signal of a continuous transition. Finally, we calculated the nearest-neighbor and next nearest-neighbor spin-spin correlations as a function of interaction. We observed a paramagnetic metallic state in the weak-coupling regime. When the interaction passes the critical point, both nearest-neighbor and next nearest-neighbor spin-spin correlations are rapidly increasing. In the strong-coupling regions the system shows the AF Mott insulator state. We did not observe a spin liquid state (paramagnetic Mott insulator) at lower temperature. However, from our calculation we expect that a continuous Mott transition with reentrant behavior will be observed experimentally.

We would like to thank A. J. Millis for helpful discussions.

- ¹ Y. Okamoto, M. Nohara, H. Aruga-katori, and H. Takagi, Phys. Rev. Lett. **99**, 137207 (2007).
- ² M. Lawler, A. Paramakanti, Y. B. Kim, and L. Balents, cond-mat/08064395.
- ³ G. Chen and L. Balents, Phys. Rev. B **78**, 094403 (2008).
- ⁴ M. Lawler, H.-Y. Kee, Y. B. Kim, and A. Vishwanath, Phys. Rev. Lett. **100**, 227201 (2008).
- ⁵ J. Hopkinson, S. Isakov, H.-Y. Kee, and Y. B. Kim, Phys. Rev. Lett. **99**, 037201 (2007).
- ⁶ Y. Zhou, P. A. Lee, T.-K. Ng, and F.-C. Zhang, Phys. Rev. Lett. **101**, 197201 (2008).
- ⁷ H. Takagi, unpublished.
- ⁸ W. Metzner and D. Vollhardt, Phys. Rev. Lett. **62**, 324 (1989).
- ⁹ A. Georges, G. Kotliar, W. Krauth, and M. Rozenberg, Rev. Mod. Phys. **68**, 13 (1996).
- ¹⁰ N. Bulut, W. Koshibae, and S. Maekawa, Phys. Rev. Lett. **95**, 037001 (2005).
- ¹¹ K. Aryanpour, W. Pickett, and R. Scalettar, Rev. Rev. B **74**, 085117 (2006).
- ¹² T. Maier, M. Jarrell, T. Pruschke, and M. Hettler, Rev. Mod. Phys. **77**, 1027 (2005).
- ¹³ M. Hettler, A. Tahvildar-zadeh, M. Jarrell, T. Pruschke, and H. Krishnamurthy, Phys. Rev. B **58**, R7475 (1998).
- ¹⁴ M. Hettler, M. Mukherjee, M. Jarrell, and H. Krishnamurthy, Phys. Rev. B **61**, 12739 (2000).
- ¹⁵ G. Kotliar, S. Savrasov, G. Palsson, and G. Biroli, Phys. Rev. Lett. **87**, 186401 (2001).
- ¹⁶ A. Rubtsov, V. Savkin, and A. Lichtenstein, Phys. Rev. B **72**, 035122 (2005).
- ¹⁷ J. Hirsch and R. Fye, Phys. Rev. Lett. **56**, 2521 (1986).
- ¹⁸ T. Ohashi, T. Momoi, H. Tsunetsugu, and N. Kawakami, Phys. Rev. Lett. **100**, 076402 (2008).
- ¹⁹ S. L. et al, Phys. Rev. Lett. **85**, 5420 (2000).
- ²⁰ F. Kagawa, T. Itou, K. Miyagawa, and K. Kanoda, Phys. Rev. B **69**, 064511 (2004).
- ²¹ T. Ohashi, N. Kawakami, and H. Tsunetsugu, Phys. Rev. Lett. **97**, 066401 (2006).
- ²² S. Moukouri and M. Jarrell, Phys. Rev. Lett. **87**, 167010 (2001).
- ²³ E. Gull, P. Werner, M. Troyer, and A. Millis, cond-mat/08053778.
- ²⁴ M. Rozenberg, R. Chitra, and G. Kotliar, Phys. Rev. Lett. **83**, 3498 (1999).
- ²⁵ D. Podolsky, A. Paramakanti, Y. B. Kim, and T. Senthil, cond-mat/0811.2218.